# Structural and magnetic properties of the iron-containing langasite family $A_3MFe_3X_2O_{14}$ ($A$ = Ba, Sr; $M$ = Sb, Nb, Ta; $X$ = Si, Ge) observed by Mössbauer spectroscopy

I. S. Lyubutin,[1] P. G. Naumov,[1] B. V. Mill',[2] K. V. Frolov,[1,*] and E. I. Demikhov[3]

[1]*Shubnikov Institute of Crystallography, Russian Academy of Sciences, 119333, Moscow, Russia*

[2]*Moscow State University, Physical Department, 119992, Moscow, Russia*

[3]*Lebedev Physical Institute, Russian Academy of Sciences, 119991, Moscow, Russia*

(Received 20 June 2011; revised manuscript received 27 November 2011; published 19 December 2011)

The occurrence of the long-range magnetic order of high-spin $Fe^{3+}$ ions is found in iron-containing langasite family crystals $A_3MFe_3X_2O_{14}$ ($A$ = Ba, Sr; $M$ = Sb, Nb, Ta; $X$ = Si, Ge) at $T \leqslant 40$ K. The Neel temperature ($T_N$) values (27.1–37.1 K) depend on the composition and significantly increase with the strengthening covalence of Fe-O bonds in the $3f$ tetrahedra. Splitting of iron positions into two magnetic sublattices is established in $Ba_3TaFe_3Si_2O_{14}$ and $Ba_3NbFe_3Si_2O_{14}$ crystals at $T < T_N$. Iron magnetic moments in two sublattices are directed at different angles to the local crystal axes with a mean value $\approx 45^\circ$. At the temperatures between 4.2 and 20 K, the iron spins in two sublattices rotate in opposite directions. It can be related to magnetic chirality in the helicoidal magnetic structure. The appearance of nonequivalent $Fe^{3+}$ sites is associated with the structural phase transition $P321 \rightarrow P3$ (or $P321 \rightarrow C2$) induced by the magnetic transition. The presence of the polar threefold axis at this transition provides the conditions for the occurrence of the ferroelectric state. Such crystals can be considered as magnetically induced multiferroics.

DOI: 10.1103/PhysRevB.84.214425 PACS number(s): 75.30.Et, 75.50.−y, 76.80.+y, 71.27.+a

## I. INTRODUCTION

Compounds with a $Ca_3Ga_2Ge_4O_{14}$-type crystal structure (space group [sp. gr.] $P321$, $Z = 1$)[1] attract great attention because of unique piezoelectric properties that exceed those of quartz as well as interesting combinations of luminescent, laser, and nonlinear optical properties.[2] Because of wide isomorphism, about 200 compounds of this type have been synthesized. A number of single crystals was also obtained by the Chokhralsky method including langasite, $La_3Ga_5SiO_{14}$, which gave the name to the whole family.[1] The possibility of synthesizing such compounds containing magnetic ions is of great interest. Supposed coexistence of electric and magnetic order parameters in such materials could provide for the creation of a new class of multiferroics. The first attempt to obtain such a magnetic compound was carried out by substituting $La^{3+}$ ions in langasite for $Nd^{3+}$ or $Pr^{3+}$ ions.[3] However, the magnetic measurements did not show any long-range order down to ultralow temperatures of 45 mK. An inelastic neutron scattering in $Nd_3Ga_5SiO_{14}$ showed a magnetic excitation resembling a spin-liquid state in the anisotropic Kagome lattice of $Nd^{3+}$ ions.[4,5]

Furthermore, attention was concentrated on the compounds containing 3d ions. The materials with paramagnetic iron ions $A_3^{2+}M^{5+}Fe_3X_2^{4+}O_{14}$ ($A$ = Ba, Sr, Ca; $M$ = Sb, Nb, Ta; $X$ = Si, Ge)[1] as well with cobalt and manganese ions $Pb_3Te^{6+}M_3^{2+}X_2^{5+}O_{14}$ ($M$ = Co, Mn; $X$ = P, V, As)[6] were synthesized by a co-author of the present study [B.V.M.'] (see also Ref. 17). The measurements of magnetic susceptibility indicate an antiferromagnetic ordering in a number of these compounds at temperatures of 7–38 K.[7–9] Recently, the neutron diffraction studies of the $Ba_3NbFe_3Si_2O_{14}$ crystal[8,10] revealed that the magnetic moments of the Fe ions were ordered at low temperatures in the $ab$ plane, and when alternating $ab$ layers along the $c$ axis, the magnetic vector rotates from one layer to another forming a helical magnetic structure. Splitting of crystallographic iron sites into two sublattices, found by Mössbauer spectroscopy in the $Ba_3TaFe_3Si_2O_{14}$ crystal,[11] can be associated with the structural phase transition induced by the magnetic ordering at $T < 27$ K.

The $Ca_3Ga_2Ge_4O_{14}$-type noncentrosymmetric trigonal structure consists of tetrahedral layers, parallel to the $ab$ plane and separated along the $c$ axis, with the layers consisting of oxygen octahedra and large polyhedra (Fig. 1).[1,12,13] There are two types of tetrahedral sites: the larger-sized tetrahedra (the central $3f$ position with symmetry 2) and the smaller-sized tetrahedra (the $2d$ position with symmetry 3). The octahedral positions $1a$ have symmetry 32. The octahedral and tetrahedral sites are occupied by $Ga^{3+}$ and $Ge^{4+}$ ions, whereas the structural holes of the framework are occupied by large ions such as $Na^+$, $Ca^{2+}$, $Sr^{2+}$, $Ba^{2+}$, $Pb^{2+}$, $La^{3+}$. The coordination polyhedron of these cations has eight oxygen vertices and can be represented as a distorted Thompson cube (the central position $3e$ with symmetry 2).

In this research, the magnetic properties of several iron-containing crystals of the langasite family $A_3MFe_3X_2O_{14}$ ($A$ = Ba, Sr; $M$ = Sb, Nb, Ta; $X$ = Si, Ge) are studied by low-temperature $^{57}$Fe-Mössbauer spectroscopy. All compounds reveal the occurrence of long-range magnetic ordering at $T \leqslant 40$ K. Splitting of iron sites into two magnetic sublattices whose magnetic moments rotate in opposite directions with temperature change, is established in $Ba_3TaFe_3Si_2O_{14}$ and $Ba_3NbFe_3Si_2O_{14}$ below the temperature of the magnetic phase transition.

## II. EXPERIMENTAL

Polycrystalline compounds of the iron-containing langasite family $Ba_3SbFe_3Si_2O_{14}$, $Ba_3SbFe_3Ge_2O_{14}$, $Ba_3NbFe_3Si_2O_{14}$, $Ba_3TaFe_3Si_2O_{14}$, and $Sr_3SbFe_3Si_2O_{14}$ were synthesized by solid-phase sintering from compacted mixtures of corresponding salts and oxides.[9] The phase composition was controlled by x-ray powder diffraction, as well as by Mössbauer

 

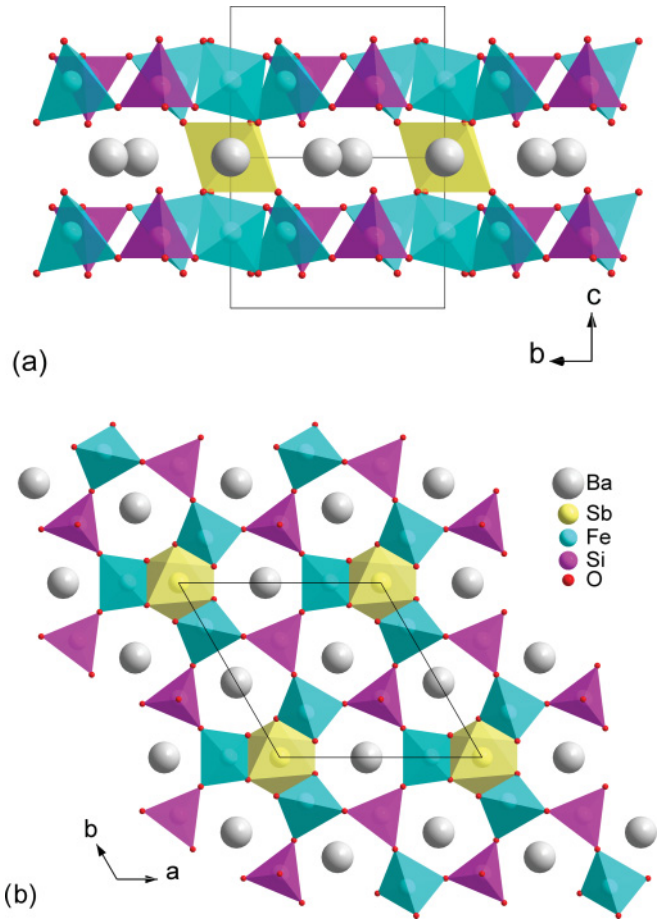


FIG. 1. (Color online) The trigonal structure of $Ba_3SbFe_3Si_2O_{14}$ (shown on the basis of the $Ca_3Ga_2Ge_4O_{14}$-type structure) projected along the $c$ axes (a) and in the $a$-$b$ plane (b). The $Sb^{5+}$ ions are inside the oxygen octahedra. The triangular clusters of $Fe^{3+}$ polyhedra can be seen in the $a$-$b$ projection (b).

spectroscopy. The single-phase samples with a $Ca_3Ga_2Ge_4O_{14}$ type structure were obtained for all compositions. The room temperature unit cell parameters are listed in Table I.

The $^{57}$Fe-Mössbauer spectra were recorded in the temperature range 4.2 to 300 K using a special closed-cycle cryostat.[14] The measurements were performed in the transmission geometry with a standard spectrometer operating in the constant acceleration regime. The gamma ray source $^{57}$Co(Rh) was located out of the cryostat. The isomer shifts were measured relative to metal $\alpha$-Fe at room temperature.

## III. EXPERIMENTAL RESULTS

### A. Paramagnetic temperature range

At room temperature, the Mössbauer spectra of all samples consist of one quadrupole doublet with narrow symmetrical resonance lines (Fig. 2). This indicates that iron ions occupy only one type of crystallographic position. The hyperfine interaction parameters (i.e., quadrupole splitting, $\Delta$, and isomer shift of resonance lines, $\delta$), are listed in Table I, and their values are characteristics of the high-spin (HS) state of $Fe^{3+}$ ions in the tetrahedral oxygen environment. As the result of crystallographic data,[6] $Fe^{3+}$ ions should occupy the larger sized $3f$ tetrahedra from two possible $3f$ and $2d$ tetrahedral positions in the langasite structure. The value $\Delta = 1.2$ to 1.3 mm/s is too large for the $S$-state $^6A_{1g}$ of $Fe^{3+}$ ions ($3d^5$) that points to a strong distortion of the [$FeO_4$] tetrahedra. The relatively low $\delta$ value is indicative of strong covalence of Fe-O chemical bonds, which implies a partial delocalization of the iron $3d$ electrons.

The doublet character of spectra is retained at temperatures decreasing from 300 to 40 K (Fig. 2). The $\delta$ parameter gradually increases in accordance with the second-order Doppler effect (the temperature shift),[15] and the $\Delta$ parameter increases slightly. Such behavior of $\delta$ and $\Delta$ points to an absence of any structural phase transitions in this temperature range. Taking into account that the resonance line area $S$ is proportional to the Mössbauer effect probability $f'$, we approximated the experimental dependences $S(T)$ to the Debye relation,[16]

$$f'(T) = \exp\left[-\frac{6E_r}{k\theta_D}\left(\frac{1}{4} + \left(\frac{T}{\theta_D}\right)^2 \int_0^{\frac{\theta_D}{T}} \frac{t\,dt}{e^t - 1}\right)\right], \quad (1)$$

where $E_r = \frac{E_\gamma^2}{2Mc^2}$ is the recoil energy in gamma resonance, $E_\gamma$ is the energy of Mössbauer gamma rays, $M$ is the mass of iron ions, $k$ is the Boltzman constant, and $c$ is the velocity of light. We applied a numerical method to fit Eq. (1) to the experimental data. The estimated values of the "Mössbauer" Debye temperatures, $\theta_D$, for the local sites of $Fe^{3+}$ ions are shown in Table I for all crystals studied.

TABLE I. The unit cell parameters ($a$, $c$) and the room temperature hyperfine parameters $\delta$, $\Delta$, and $\Gamma_{exp}$ of the iron-containing langasites obtained from the Mössbauer spectrum. $\delta$ is the isomer shift (relative to $\alpha$-Fe at 300 K), $\Delta = e^2qQ/2$ is the quadrupole splitting, $\Gamma_{exp}$ is the half-maximum line width, $T_N$ is the Neel temperature, $\varphi$ is the average value of the angle between the iron magnetic moment and local EFG axis, and $\theta_D$ is the Debye temperature.

| Compound | $a$ (Å) | $c$ (Å) | $\delta$ (mm/s) | $\Delta$ (mm/s) | $\Gamma_{exp}$ (mm/s) | $T_N$ (K) | $\varphi$ (degree) | $\Theta_D$ (K) |
|---|---|---|---|---|---|---|---|---|
| | ±0.001 | ±0.001 | ±0.005 | ±0.005 | ±0.005 | ±0.1 | ±1 | ±10 |
| $Sr_3SbFe_3Si_2O_{14}$ | 8.304 | 5.154 | 0.210 | 1.181 | 0.347 | 37.1 | 43 | 310 |
| $Ba_3SbFe_3Si_2O_{14}$ | 8.517 | 5.252 | 0.226 | 1.281 | 0.298 | 36.1 | 44 | 230 |
| $Ba_3SbFe_3Ge_2O_{14}$ | 8.628 | 5.277 | 0.229 | 1.274 | 0.312 | 35.0 | 42 | 220 |
| $Ba_3TaFe_3Si_2O_{14}$ | 8.539 | 5.234 | 0.239 | 1.252 | 0.324 | 27.2 | 45 | 280 |
| $Ba_3NbFe_3Si_2O_{14}$ | 8.525 | 5.239 | 0.242 | 1.242 | 0.356 | 27.1 | 45 | 300 |

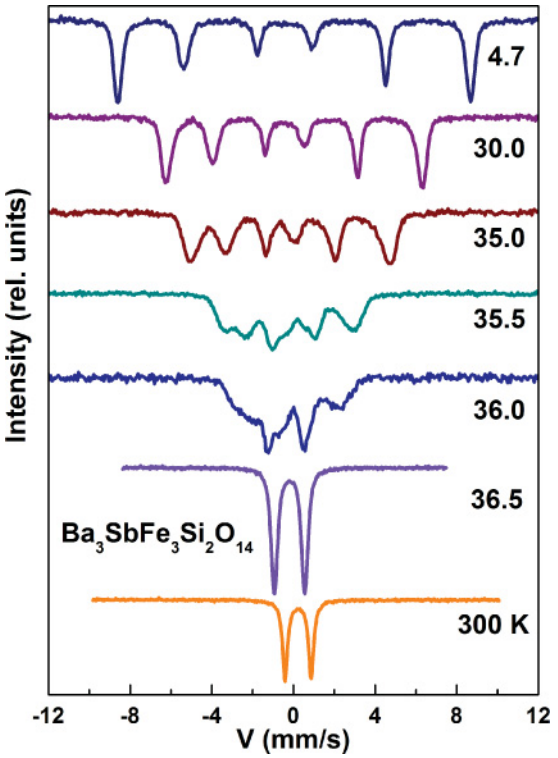


FIG. 2. (Color online) The $^{57}$Fe-Mössbauer spectra of $Ba_3SbFe_3Si_2O_{14}$ at several selected temperatures in the region of the magnetic transition and at room temperature.

### B. Low temperature range

A further temperature decrease leads to splitting of the Mössbauer spectra into six Zeeman components typical of the magnetic ordering of iron ions (Figs. 2 and 3). The temperatures of a magnetic phase transition are different for various sample compositions, and they are within the limits of ~27–37 K (see Table I). From the values of magnetic hyperfine splitting of Mössbauer lines, we calculated the values of magnetic hyperfine fields $H_{hf}$ at iron nuclei; their temperature dependences are shown in Fig. 4. It is established that the $H_{hf}$ dependences are typical of three-dimensional magnetic ordering, and the transition into the paramagnetic state near the Neel temperature ($T_N$) is the second-order transition. A negative value of the paramagnetic Curie point obtained in the similar crystals[9,17] points to an antiferromagnetic ordering character. Supposing a proportionality between the $H_{hf}$ value and the magnetic moment of $Fe^{3+}$ ions, we approximated the $H_{hf}(T)$ dependence near $T_N$ with the equation for critical indices

$$H_{hf}/H_0 = (1 - T/T_N)^{\beta}, \quad (2)$$

where $H_0 = H_{hf}$ $(T = 0)$. The example of such approximation of experimental data for the $Ba_3NbFe_3Si_2O_{14}$ compound is shown in the inset to Fig. 4. The $T_N$ values obtained in this way are listed in Table I, whereas the values of critical indices $\beta$ for all samples are the same 0.30 (±0.02) within the limit of error. According to theory,[18,19] the value $\beta = 0.30$ is a typical characteristic of the 3D Heisenberg magnet.

Analysis of the parameters in Table I shows that the $T_N$ value for three compounds with $Sb^{5+}$ ions is notably higher

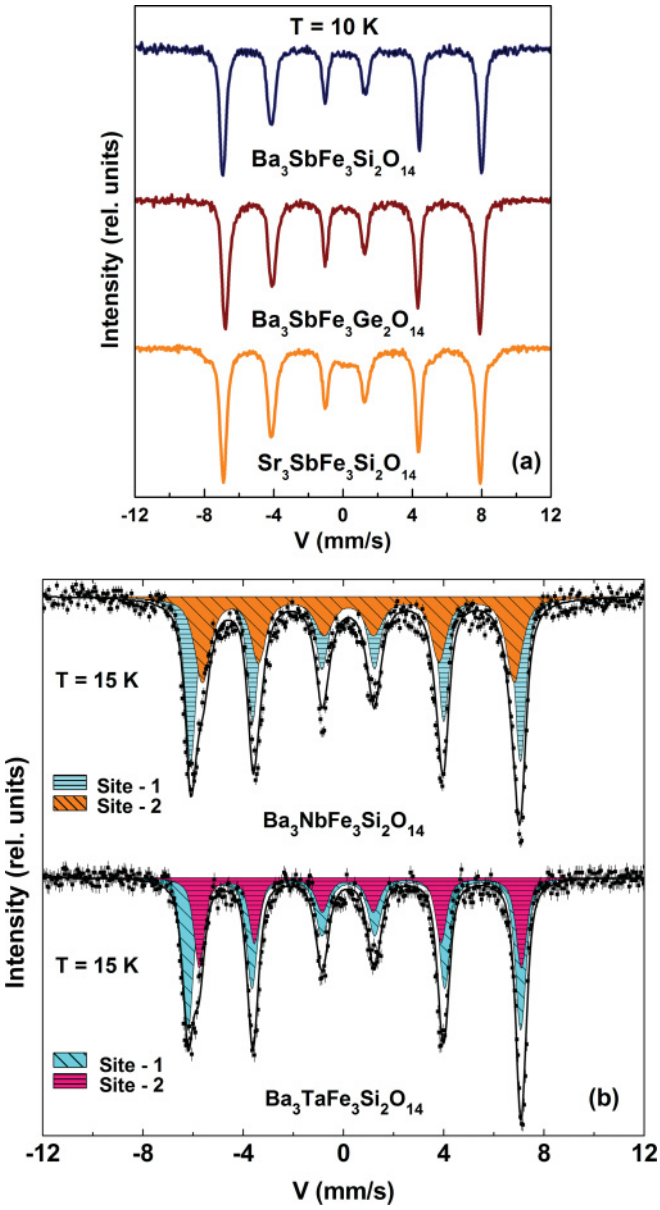


FIG. 3. (Color online) The $^{57}$Fe-Mössbauer spectra of the iron-contained langasite compounds below $T_N$ with $Sb^{5+}$ ions in octahedral sites (a) and with $Nb^{5+}$ and $Ta^{5+}$ ions (b). (a) Single six-line spectra are observed. (b) The spectra fit to two magnetic components is shown by dashed lines. Color: blue and red resonance lines correspond to the nonequivalent iron site 1 and site 2.

than the values for the compounds with $Nb^{5+}$ and $Ta^{5+}$ ions. An obvious correlation between $T_N$ and isomer shift $\delta$ values is observed in these three compounds, meaning the lower the $\delta$ (i.e., the greater the covalence of Fe-O bonds in the $3f$ tetrahedra), the greater the $T_N$ value. This tendency (for correlation between $T_N$ and $\delta$) is also traceable for all series of the five samples.

At 4.2 K, the magnetic field $H_{hf}$ is almost saturated (Fig. 4), and its value is about 46 T. Such $H_{hf}$ value is typical of the tetrahedral oxygen environment of the high-spin (HS) $Fe^{3+}$ ions with strong Fe-O covalent bonding,[20–22] which leads to a partial delocalization of iron $d$-electrons. This is also supported

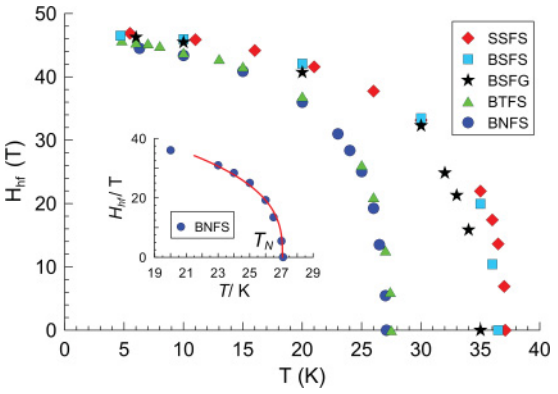


FIG. 4. (Color online) Temperature dependencies of the average magnetic hyperfine fields at Fe nuclei in $Ba_3SbFe_3Si_2O_{14}$ (BSFS), $Ba_3SbFe_3Ge_2O_{14}$ (BSFG), $Ba_3NbFe_3Si_2O_{14}$ (BNFS), $Ba_3TaFe_3Si_2O_{14}$ (BTFS), and $Sr_3SbFe_3Si_2O_{14}$ (SSFS). Solid line in inset shows an example of the approximation of experimental data for $Ba_3NbFe_3Si_2O_{14}$ to Eq. (2).

by the above mentioned isomer shift value. For comparison, the $H_{hf}$ value is ≈46.0 T for the tetrahedral $d$-sites and ≈55.0 T for the octahedral $a$-sites in yttrium iron garnet ($Y_3Fe_5O_{12}$), where $Fe^{3+}$ ions occupy both the $d$ and $a$ sites.[21,22] These data show that $Fe^{3+}$ ions occupy only the tetrahedral $3f$ sites in langasites, and they are absent in the octahedral $1a$ sites.

The value $H_{hf} \approx 55.0$ T is typical of the HS-$Fe^{3+}$ ions in octahedral coordination with an iron $3d^5$ electron configuration (spin $S = 5/2$) and a magnetic moment of $M = 5\mu_B$ per $Fe^{3+}$ ion. The relation, well-known for oxides, follows from the data that the field $H_{hf} = 11.0$ T approximately corresponds to $M = 1\mu_B$. From these estimations we can approximate the average value of an iron ion magnetic moment in langasites. Knowing the experimental value of saturation field $H_{hf} \approx 46.0$ T we obtain $M \approx 4.18\mu_B$/Fe. This value is close to that found by neutron diffraction.[17]

We found that at $T < T_N$, the value of the quadrupole parameter $\varepsilon$ (the quadrupole shift) for all crystals is essentially less than the $\Delta$ value at $T > T_N$ (Fig. 5). From the temperature behavior of the $\varepsilon$ parameter, one can obtain information about the orientation of the iron magnetic moment relative to the crystal axes. When the magnetic hyperfine interaction is much greater than the electric quadrupole interaction, the quadrupole shift $\varepsilon = (e^2qQ)_{obser}$ observed at $T < T_N$ and the true quadrupole splitting $\Delta = e^2qQ$ (which we can obtain above $T_N$) are in the relation[15,23]

$$(e^2qQ)_{obser} \approx e^2qQ\,\frac{3\cos^2\varphi - 1}{2}, \qquad (3)$$

Here, $Q$ is the nuclear quadrupole moment, $\varphi$ is the angle between the direction of iron magnetic moment and the main axis of the electric field gradient (EFG), and $eq = V_{zz} = \partial^2V/\partial z^2$. Thus, the angular dependence of $(e^2qQ)_{obser}$ can be used to define the directions of iron moment relative to crystal axes if the main axis of EFG, $V_{zz}$, is known. If the point symmetry of the $Fe^{3+}$ ion is less than threefold, the asymmetry

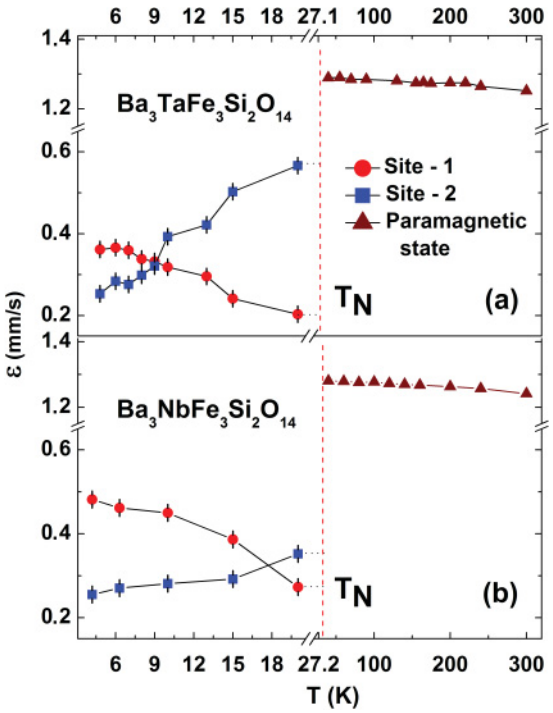


FIG. 5. (Color online) Temperature dependencies of the quadrupole shift parameters $\varepsilon$ in $Ba_3TaFe_3Si_2O_{14}$ (a) and $Ba_3NbFe_3Si_2O_{14}$ (b) for two nonequivalent iron sites at $T < T_N$ $\{\varepsilon_{1,2} = e^2qQ/2[(3\cos^2\varphi_{1,2} - 1)/2]\}$, and for a single site at $T > T_N$ ($\varepsilon = \Delta = e^2qQ/2$). Note the change of both $x$ and $y$ scales at $T_N$. Solid lines are guides for the eye.

parameter $\eta = (V_{xx} - V_{yy})/V_{zz}$ has to be taken into account in Eq. (3)

$$\varepsilon = \frac{e^2qQ}{2}\left(1 + \frac{\eta^2}{3}\right)^{1/2}, \qquad (4)$$

The values of angles $\varphi$ calculated in this way are listed in Table I. We found that in all crystals studied, the iron magnetic moments are oriented at an angle of ∼45° to a local EFG axis.

### C. Nonequivalent iron sites at $T < T_N$

An anomalous behavior of Mössbauer spectra was found in the low temperature range for two $Ba_3NbFe_3Si_2O_{14}$ and $Ba_3TaFe_3Si_2O_{14}$ crystals of the series studied [Fig. 3(a)]. The shapes of resonance lines (width and intensity) in left and right parts of the spectrum are essentially different, which signifies an appearance of several nonequivalent iron sites. The computer analysis of different models of spectra processing shows that the best approximation is reached at spectra fitting to two magnetic components [Fig. 3(b)]. The values of hyperfine interaction parameters $H_{hf}$, $\delta$, and $\varepsilon$ for iron ions in two nonequivalent sublattices at 4.2 K are given in Table II for $Ba_3TaFe_3Si_2O_{14}$.

From the value of the quadrupole shift, we have established that angle $\varphi$ between the iron magnetic moment and local EFG axis is slightly different for two iron lattices. In particular, at $T = 4.5$ K, these angles are $\varphi_1 = 44°$ (±1) and $\varphi_2 = 47°$ (±1) in $Ba_3TaFe_3Si_2O_{14}$, but they are $\varphi_1 = 40°$ (±1) and $\varphi_2 = 47°$ (±1) in $Ba_3NbFe_3Si_2O_{14}$, with the average $\varphi$ value near

TABLE II. The hyperfine parameters for two nonequivalent iron sites in $Ba_3TaFe_3Si_2O_{14}$ (BTFS) and $Ba_3NbFe_3Si_2O_{14}$ (BNFS) obtained from the Mössbauer spectrum at 4.2 K: $H_{hf}$ is the magnetic hyperfine field at $^{57}$Fe nuclei, $\varepsilon = e^2qQ/2[(3\cos^2\varphi - 1)/2]$ is the quadrupole shift at $T < T_N$, $\delta$ is the isomer shift, and $S$ is the relative area of the magnetic component.

| Fe site | $H_{hf}$ (T) (±0.1) | | $\varepsilon$ (mm/s) (±0.01) | | $\delta$ (mm/s) (±0.01) | |
|---|---|---|---|---|---|---|
| Compound | BTFS | BNFS | BTFS | BNFS | BTFS | BNFS |
| Site 1 | 45.9 | 45.4 | 0.36 | 0.48 | 0.31 | 0.25 |
| Site 2 | 44.0 | 44.1 | 0.25 | 0.26 | 0.39 | 0.38 |

45° in both crystals. It is interesting that the $\varphi$ value changes with temperature rise; moreover, it increases in one sublattice and decreases in the other (Fig. 6). In the $Ba_3TaFe_3Si_2O_{14}$ crystal, $\varphi_1(T)$ and $\varphi_2(T)$ curves intersect at $T_{reor} \approx 9$ K, and then they reach the values $\varphi_1 = 49°$ and $\varphi_2 = 38°$ at 20 K temperature (Fig. 6). Thus, a spin reorientation occurs between 4.2 and 20 K when the iron magnetic moments in two sublattices rotate through ~10° to opposite directions. A similar behavior is observed in the $Ba_3NbFe_3Si_2O_{14}$ crystal; however, the intersection point of the $\varphi_1(T)$ and $\varphi_2(T)$ curves is higher, $T_{reor} \approx 18$ K (Fig. 6). Meanwhile, the single-angle value $\varphi$ in the other three compounds—$Ba_3SbFe_3Si_2O_{14}$, $Ba_3SbFe_3Ge_2O_{14}$, and $Sr_3SbFe_3Si_2O_{14}$—is nearly constant at temperatures between 4.2 and 30 K.

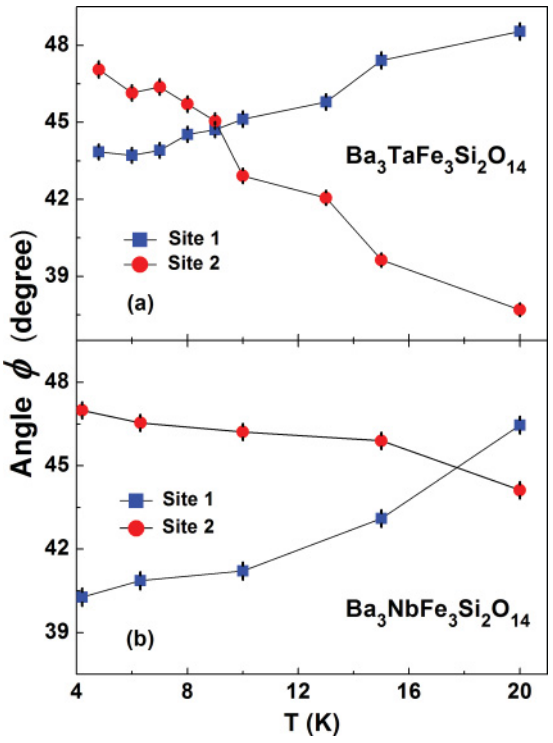


FIG. 6. (Color online) Temperature dependences of the angle $\varphi$ between Fe magnetic moments and the EFG axis of the local Fe site in $Ba_3TaFe_3Si_2O_{14}$ (a) and $Ba_3NbFe_3Si_2O_{14}$ (b) for two nonequivalent iron sites. Solid lines are guides for the eye.

## IV. DISCUSSION

### A. Exchange interactions and magnetic structure

In the $Ca_3Ga_2Ge_4O_{14}$-type structure, $Fe^{3+}$ ions occupy the $3f$ tetrahedra forming a net of triangle clusters on a hexagonal lattice in planes parallel to the $ab$ plane [Figs. 1(b) and 7(a)].[1] In the iron layers, each $Fe^{3+}$ ion is coupled by superexchange interaction with the two nearest $Fe^{3+}$ neighbors of its own triangle ($J_1$) and with the four $Fe^{3+}$ neighbors of the other three nearest triangles ($J_2$) [Fig. 7(a)].[10–12,17] Within the layer, the $J_2$ interactions are realized via two oxygens Fe-O-O-Fe, whereas the $J_1$ interactions are mediated via one oxygen Fe-O-Fe. However, one Fe-O bond in the Fe-O-Fe path is relatively short, whereas the other one is long [see Fig. 7(b) and 7(c)]. In a typical crystal,[24] the short Fe-O bond in the $J_1$ interaction is ≈1.836 Å, and the long Fe-O bond is ≈2.694 Å. In the $J_2$ interaction, the lengths of bonds are (Fe-O) ≈ 1.887 Å and (O-O) ≈ 2.777 Å.[24]

The nearest $Fe^{3+}$ layers are separated by the layers containing $A^{2+}$ and $M^{5+}$ ions, and the interlayer interactions should be also taken into account. Each $Fe^{3+}$ ion has three nearest $Fe^{3+}$ ions from the neighboring iron layer. This $Fe^{3+}$ ion is coupled with each of its neighbors via two oxygens Fe-O-O-Fe [Figs. 7(b) and 7(c)]. The geometry of these bonds and the Fe-O and O-O lengths are different (the short Fe-O

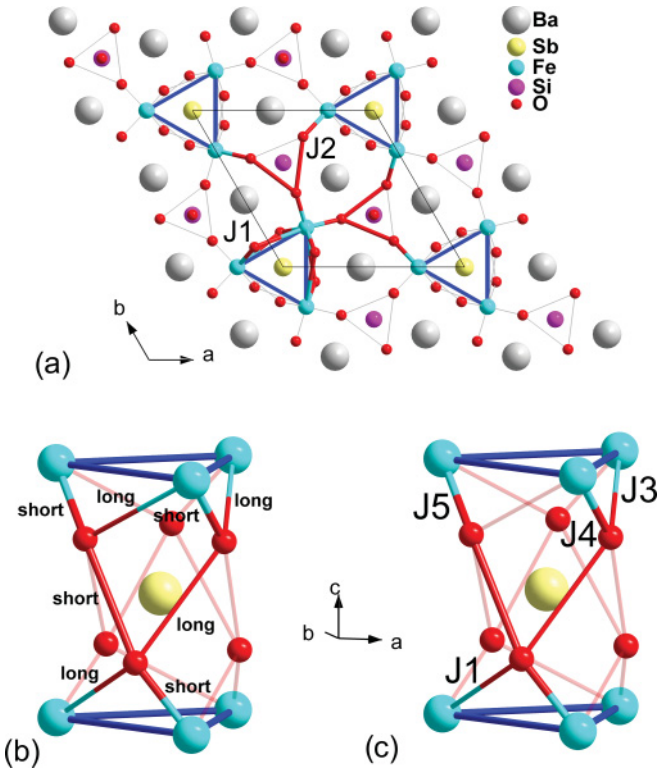


FIG. 7. (Color online) The intralayer (a) and interlayer (b, c) superexchange bonds in the trigonal structure of $Ba_3SbFe_3Si_2O_{14}$. In the $a$-$b$ projection (a), the triangle plain net of magnetic $Fe^{3+}$ ions is shown by blue/medium gray lines, and $J1$ and $J2$ indicate the in-plane superexchange Fe-O-Fe and Fe-O-O-Fe interactions (red/dark gray), respectively. (b, c) The "short" (thick) and "long" (thin) lengths of the Fe-O (blue/medium gray-red/dark gray) and O-O (red/dark gray) bonds for the interlayer $J3$, $J4$, and $J5$ interactions.

length in Fig. 7(b) is ≈1.836 Å and the long Fe-O length is ≈2.694 Å, whereas the "short" O-O length is ≈2.905 Å and the "long" O-O length is ≈3.386 Å).[24] It leads to different values of the interlayer exchange integrals $J_3$, $J_4$, and $J_5$. As shown in Fig. 7(b) and 7(c), the $J_5$ interaction is realized via the shortest path.

The competition between these interactions should, apparently, lead to a frustrated magnetic structure. We concluded from our $T_N$ values and the data on the paramagnetic Curie point $\Theta_{CW}$[11,17] that the magnetic frustration parameter $f = \Theta_{CW}/T_N$ for the crystals studied depends on their composition and is within the limits of ≈3–7. This implies a significant frustration of magnetic systems that can result in the 120° spin arrangement in the triangle lattice of iron magnetic moments. Such 120° spin ordering in the iron triangles within $ab$ layers was recently found in the neutron diffraction measurements of $Ba_3NbFe_3Si_2O_{14}$ ($f = 6.65$).[10,17] When alternating the $ab$ layers along the $c$ axis, the iron moments of each triangle rotate by ≈51°, forming a helical structure. The helical magnetic structure is incommensurate with the crystal lattice, and the helix period is near seven lattice parameters of $c$.[8]

Remarkably the helical magnetic structure with a Mn spin rotation between consecutive layers of ≈51° was found in the *b.c.* tetragonal $MnO_2$.[25] In the helical structure of $FeCl_3$, besides the spin rotation along the $c$ axis, an additional rotation by 12° was observed in the basal crystal plane.[26] This resembles a behavior of iron spins found in our $Ba_3TaFe_3Si_2O_{14}$ and $Ba_3NbFe_3Si_2O_{14}$ crystals.

In the molecular field approximation, the noncollinear spin structure and helical structures can appear as the result of a competition between several exchange interactions $J_i$ of a magnetic ion with its nearest neighbors.[27,28] According to J. Smart,[29] one can evaluate the exchange parameter using the relation between $J_i$ and the Neel temperature

$$T_N = \frac{2S(S+1)}{3k} J(q), \tag{5}$$

where $S$ is the ion spin, $k$ is the Boltzmann constant, $q$ is the propagation vector (along the $c$ axis) representing the layered magnetic structures with layers perpendicular to $q$, and $J(q)$ is the exchange interaction integral, the highest value of which determines the magnetic transition (i.e., the $T_N$ value). The $T_N$ values, which we found for the five crystals, are within the limit 27.1–37.1 K (Table I). From these data, and taking the $Fe^{3+}$ ion spin $S = 5/2$, we obtained from Eq. (5) that an average value of exchange interaction integral $|J|$ for these compounds is within the limit from ≈3.1 to ≈4.2 K.

### B. Magnetically induced structural transition

In the $Ba_3TaFe_3Si_2O_{14}$ and $Ba_3NbFe_3Si_2O_{14}$ compounds, the Mössbauer data reveal two nonequivalent sites for iron ions at $T < T_N$ and one site at $T > T_N$. This effect is, apparently, associated with the structural phase transition which is induced by the magnetic transition. The possible structural transitions in langasite family crystals were considered and observed experimentally in Ref. 30. In particular, the change of trigonal symmetry (sp. gr. $P321$) into monoclinic symmetry (sp. gr. $A2$–$C2$) was found in $La_3SbZn_3Ge_2O_{14}$ with a decrease in temperature, as well in $La_3Nb_{0.5}Ga_{5.5}O_{14}$ and $La_3Ta_{0.5}Ga_{5.5}O_{14}$ crystals under the action of high pressure.[30] It was shown that the transitions with decreasing symmetry $P321 \rightarrow P3$ and $P321 \rightarrow C2$ are most probable in the langasite family. In the first transition, the twofold axes are lost, and in the second transition, the threefold axis disappears. The loss of the threefold axis and two (of three) twofold axes at the $P321 \rightarrow C2$ transition results in splitting of the $3e$ and $3f$ sites (the $Ba^{2+}$ and $Fe^{3+}$ ions in this case). The remaining twofold axis becomes polar, thus creating the conditions for the appearance of a ferroelectric state. At least two order parameters appear in such a crystal, and it becomes a multiferroic one.

The occupancy of two nonequivalent $3f$ sites in the monoclinic phase $C2$ follows the ratio 1:2, which correlates with our Mössbauer data for the $Ba_3TaFe_3Si_2O_{14}$ crystal. Thus, one can suppose that the appearance of two nonequivalent iron sites in $Ba_3TaFe_3Si_2O_{14}$ and $Ba_3NbFe_3Si_2O_{14}$ at low temperatures is caused by the structural phase transition from the trigonal $P321$ phase to the monoclinic $C2$ phase, which is induced by the magnetic transition. In this case, these crystals can be considered magnetically induced multiferroics.

The measurement of electric polarization in the $Ba_3NbFe_3Si_2O_{14}$ single crystal[31] revealed at $T < T_N$ an appearance of polarization along the $c$ axis, which is the threefold axis in the space group $P3$. Apparently, this result does not support our assumption of a $P321 \rightarrow C2$ transition, since electric polarization in the space group $C2$ ($A2$) should be directed along polar axis 2, which is normal to the threefold axis in the space group $P321$.[12] Recently, a possible structural transition from the $P321$ to $P3$ phase associated with the magnetic transition was supposed in the $Ba_3NbFe_3Si_2O_{14}$ crystal.[17] At such a transition, the twofold axes disappear, and $Fe^{3+}$ ions remain in the equivalent positions.

Nevertheless, within the framework of symmetry $P3$ having a metric of the cell close to $P321$ ($Z = 1$), one may allow splitting of $Fe^{3+}$ sites into two positions with a common occupancy equal to unity. These positions would be at the short distance (∼0.2–0.5 Å) apart, which can be temperature dependent. Filling of these two split positions is not determined. Both iron sublattices can take part in the formation of a magnetic helix[11] with a slightly different behavior from $Fe^{3+}$ magnetic moments in two sublattices. The split iron positions can be distributed randomly in the crystal lattice as unit cells with single type of iron sites. This makes difficult the detection of a such structure by the x-ray method. To clarify these effects, the careful structural studies of single crystals are necessary at low temperatures.

## V. CONCLUSIONS

The appearance of the long-range 3D magnetic order of high-spin $Fe^{3+}$ ions in the tetrahedral $3f$ positions is found in five crystals of the iron-containing langasite family $A_3MFe_3X_2O_{14}$ ($A$ = Ba, Sr; $M$ = Sb, Nb, Ta; $X$ = Si, Ge) at $T \leqslant 40$ K. The $T_N$ values quite strongly depend on the composition, and they are within the limit 27.1–37.1 K, whereas the values of iron ion magnetic moments evaluated from the Mössbauer data are $\approx 4.2 \mu_B$/Fe. The correlation between $T_N$ and the isomer shift $\delta$ is established, which reveals that the $T_N$ value significantly increases with the strengthening

covalence of Fe-O bonds in the $3f$ tetrahedra. In particular, the $T_N$ value for compounds with $Sb^{5+}$ ions in $1a$ octahedra is about 30% higher than in the compounds with $Nb^{5+}$ and $Ta^{5+}$.

Splitting of iron sites into two magnetic sublattices is established in the $Ba_3NbFe_3Si_2O_{14}$ and $Ba_3TaFe_3Si_2O_{14}$ crystals below the temperature of magnetic phase transition. The iron moments in two sublattices are directed at different angles to the local crystal axes with the mean value $\sim 45^\circ$. With a temperature rise from 4.2 to 20 K, the magnetic moments of two sublattices rotate in opposite directions. The effect of spin reorientation may be related to the magnetic chirality in the helicoidal magnetic structure. The nonequivalent positions originate from the structural phase transition induced by the magnetic transition. The trigonal $P321$ structure can transform either to the $P3$ or monoclinic $C2$ structure. The appearance of the polar threefold axis at such a transition creates the conditions for the ferroelectric state, and such crystals can be considered magnetically induced multiferroics. A spontaneous electric polarization observed in $Ba_3NbFe_3Si_2O_{14}$ at $T < T_N$[31] demonstrates the relation between the electric and magnetic order parameters in the iron-containing langasite family materials.

## ACKNOWLEDGMENTS

This work is supported by the Russian Foundation for Basic Research Grants No.11-02-00636a, No. 09-02-00444a, and No. 11-02-12089 and by the "Strongly correlated electronic systems" program of the Russian Academy of Sciences.

*green@ns.crys.ras.ru

[1] B. V. Mill, E. L. Belokoneva, and T. Fukuda, Russian J. Inorg. Chem. **43**, 1168 (1998).
[2] B. V. Mill and Yu. V. Pisarevsky, in *Proceedings of the 2000 IEEE/EIA International Frequency Control Symposium* (Kansas City, MO, 2000), p. 133.
[3] P. Bordet, I. Gelard, K. Marty, A. Ibanez, J. Robert, V. Simonet, B. Canals, R. Ballou, and P. Lejay, J. Phys. Condens. Matter **18**, 5147 (2006).
[4] J. Robert, V. Simonet, B. Canals, R. Ballou, P. Bordet, P. Lejay, and A. Stunault, Phys. Rev. Lett. **96**, 197205 (2006).
[5] J. Robert, V. Simonet, B. Canals, R. Ballou, P. Bordet, I. Gelard, A. Ibanez, P. Lejay, J. Ollivier, and A. Stunault, Physica B **385-386**, 72 (2006).
[6] B. V. Mill', Russian J. Inorg. Chem. **54**, 1205 (2009).
[7] V. Yu. Ivanov, A. A. Mukhin, A. S. Prokhorov, and B. V. Mill, in *Proceedings of the Moscow International Symposium on Magnetism* (Moscow State University, Moscow, Russia, 2008), p. 601.
[8] K. Marty, V. Simonet, E. Ressouche, R. Ballou, P. Lejay, and P. Bordet, Phys. Rev. Lett. **101**, 247201 (2008).
[9] V. Yu. Ivanov, A. A. Mukhin, A. S. Prokhorov, and B. V. Mill, Solid State Phenomena **152-153**, 299 (2009).
[10] K. Marty, V. Simonet, P. Bordet, R. Ballou, P. Lejay, O. Isnard, E. Ressouche, F. Bourdarot, and P. Bonville, J. Magn. Magn. Mater. **321**, 1778 (2009).
[11] I. S. Lyubutin, P. G. Naumov, and B.V. Mill', Euro. Phys. Lett. **90**, 67005 (2010).
[12] E. L. Belokoneva and N. V. Belov, Dokl. Akad. Nauk SSSR **260**, 1363 (1981).
[13] B. V. Mill, A. V. Butashin, G. G. Kodzhabagyan, E. L. Belokoneva, and N. V. Belov, Dokl. Akad. Nauk SSSR **264**, 1395 (1982).
[14] P. G. Naumov, I. S. Lyubutin, K. V. Frolov, and E. I. Demikhov, Instrum. Exp. Tech. **53**, 770 (2010).
[15] G. K. Wertheim, *Mossbauer Effect. Principles and Applications* (Academic, New York and London, 1964), p. 38.
[16] E. Cotton, J. Phys. Radium **21**, 265 (1960).
[17] K. Marty, P. Bordet, V. Simonet, M. Loire, R. Ballou, C. Darie, J. Kljun, P. Bonville, O. Isnard, P. Lejay, B. Zawilski, and C. Simon, Phys. Rev. B **81**, 054416 (2010).
[18] L. J. De Jongh, in *Magnetic Properties of Layered Transition Metal Compounds*, edited by L. J. de Jongh (Kluver Academic Publishers, Netherlands, 1990), p. 1.
[19] J.-P. Renard, in *Organic and Inorganic Low-Dimensional Crystalline Materials*, edited by P. Delhaes and M. Drillon (Plenum Press, New York, London, 1987), p. 125.
[20] I. S. Lyubutin, in *Proceedings of the International Conference on the Application of the Mössbauer Effect* (Hungarian Academy of Sciences, Tihany, Hungary, 1969), p. 467.
[21] I. S. Lyubutin, E. F. Makarov, and V. A. Povitskii, J. Symp. Faraday Soc. **1**, 31 (1967).
[22] I. S. Lyubutin, E. F. Makarov, and V. A. Povitskii, Zh. Eksp. Teor. Fiz. **53**, 65 (1968) [Sov. Phys. JETP **26**, 44 (1968)].
[23] N. N. Greenwood and T. C. Gibb, *Mossbauer Spectroscopy* (Chapman and Hall. Ltd., London, 1978).
[24] A. A. Pugacheva, B. A. Maksimov, B. V. Mill', Yu. V. Pisarevskii, D. F. Kondakov, T. S. Chernaya, I. A. Verin, V. N. Molchanov, and V. I. Simonov, Cryst. Rep. **49**, 70 (2004).
[25] A. Herpin, P. Meriel, and A. Meyer, Comp. Rend. **246**, 3170 (1958).
[26] J. W. Cable, M. K. Wilkinson, E. O. Wollan, and W. C. Koehler, Phys. Rev. **127**, 714 (1962).
[27] D. I. Khomskii, J. Magn. Magn. Mater. **306**, 1 (2006).
[28] D. I. Khomskii, Physics **2**, 20 (2009).
[29] J. S. Smart, *Effective Field in Theories of Magnetism* (W.B. Saunders Company, Philadelphia, London, 1966), pp. 125–215.
[30] B. V. Mill', B. A. Maksimov, Yu. V. Pisarevsky, N. P. Daniliva, A. Pavlovska, S. Werner, and J. Schneider, Cryst. Rep. **49**, 60 (2004).
[31] H. D. Zhou, L. L. Lumata, P. L. Kuhns, A. P. Reyes, E. S. Choi, N. S. Dalal, J. Lu, Y. J. Jo, L. Balicas, J. S. Brooks, and C. R. Wiebe, Chem. Mater. **21**, 156 (2009).